JOURNAL OF APPLIED ELECTROCHEMISTRY 18 (1988) 731–738

Aluminium dissolution in $NaF–AlF_3–Al_2O_3$ systems

E. SUM, M. SKYLLAS-KAZACOS

School of Chemical Engineering and Industrial Chemistry, University of New South Wales, PO Box 1, Kensington, NSW 2033, Australia

Received 24 November 1987; revised 17 March 1988

The rate of dissolution of electrolytically deposited aluminium was determined by the method of current reversal chronopotentiometry at a tungsten electrode in $NaF–AlF_3–Al_2O_3$ melts of varying NaF/AlF_3 molar ratios or cryolite ratios (CR). The temperature was maintained at 1031 ± 3° C and the alumina content at 4 wt %. More accurate data were obtained by introducing delay times of various lengths (at zero current) between the cathodic and anodic current pulses, compared to direct current reversal chronopotentiometry with varying forward (deposition) times. The rate of aluminium dissolution increased with increasing NaF/AlF_3 molar ratio, the curve showing an inflexion in the vicinity of CR = 3. This inflexion indicates two dissolution mechanisms, one being predominant depending on the CR. The main reaction in acidic melts (CR < 3) may be represented by

$$2Al(l) + AlF_6^{3-} \rightleftharpoons 3Al(I)F_x^{(1-x)} + (6 - 3x)F^-$$

while in basic melts (CR > 3)

$$Al(l) + 3Na^+ \rightleftharpoons 3Na(soln) + Al(III)$$

is the likely dominant mechanism. For 0.8 < CR < 5.7 the rate of dissolution is of the order of 10^{-7} mol $cm^{-2} s^{-1}$.

1. Introduction

In the Hall–Heroult process, liquid aluminium is deposited at the cathode and carbon dioxide is evolved at the consumable carbon anode during the electrolysis of molten cryolite. Modern Hall–Heroult cells operate between 85 and 92% current efficiency [1], the main reaction responsible for the losses being the reoxidation of dissolved metal [1–3]:

$$2Al(soln) + 3CO_2 \rightleftharpoons Al_2O_3 + 3CO \quad (1)$$

which is also known as the 'back reaction'.

Although the rate determining step in the overall mechanism of the back reaction is still unclear, in general, it appears to be mass transfer or reaction controlled under condition of limited stirring or convection. Where there is vigorous agitation of the bath, the controlling step seems to be diffusion through the bath/metal interface or metal dissolution [3].

In industrial cells, turbulence in the bath resulting from magnetic fields and gas bubbles would lead to metal dissolution being rate determining in the back reaction [2].

There has been little published on the rate of aluminium dissolution in cryolite systems, although many workers have investigated the saturation solubility of aluminium as well as the dissolution reaction itself. Oblakowski and Orman [4] studied the dissolution rate of aluminium in cryolite–10% Al_2O_3 at 1000° C with and without stirring with CO_2, air or argon. The Al losses were determined by taking samples of the melt at regular time intervals and measuring the concentration of elemental Al by electron microprobe analysis. The problems with this method are possible losses during quenching of the sample and ignoring the concentration of dissolved metal in the form of sodium species. Bersimenko and Vetyukov [5] determined the rate of aluminium loss from the rate of pressure change in an airtight retort where the products formed by dissolution of aluminium in the cryolite–alumina melt interacted with oxygen. In another report by the same workers [6], they studied the rate of aluminium loss with the aid of kinetic curves of aluminium weight decrease and oxygen pressure change in a sealed retort. Kinetic curves for metal weight losses were obtained by bubbling carbon monoxide through the melt and determining the concentration of sooty carbon formed. In a separate publication, Bersimenko [7] showed that the rate of aluminium weight loss did not depend on the oxidation ability of the gas bubbling through the melt (O_2, CO_2 or CO), and that the oxidation of dissolved metal was not rate determining in the mechanism of aluminium loss under the conditions of the experiment. In their experiments, the authors would have had to assume that the reaction

$$2Al(soln) + 3CO(g) \longrightarrow Al_2O_3 + 3C(s) \quad (2)$$

was complete and that all carbon formed was detected. The method of carbon content determination was not described in Ref. [6]. The other problem with the experimental set-up was the measurement of oxygen pressure changes. The apparatus would have to be perfectly sealed and the errors are likely to be large

0021-891X/88 $03.00 + .12

since the pressure changes resulting from the interaction of products of dissolution of aluminium with oxygen are small.

A recent publication by Duruz and Landolt [8] showed that aluminium deposition and dissolution in cryolite melts of various composition could be studied by potential sweep and galvanostatic techniques at a tungsten electrode. In a previous paper [9] they showed, by scanning electron microscopy and microprobe analysis, that alloy formation resulted from the dissolution of tungsten into the deposited aluminium. Although alloy formation occurred [8–11], voltammograms exhibiting deposition and stripping of aluminium were reproducible [8–10]. The results of Duruz *et al.* [9] were qualitative and they did not show quantitatively how the dissolution rate varied with electrolyte composition.

The aims of this investigation are to determine the rates of dissolution of deposited aluminium for cryolite melts with 4 wt % alumina but varying in the cryolite ratio (CR = moles NaF/moles AlF_3), and to examine the mechanism of dissolution of aluminium. The tungsten electrode was chosen because other metal electrodes such as nickel, platinum, gold, rhodium and iridium [9, 10] greatly influence the deposition and oxidation of aluminium due to alloy formation, and carbon electrodes such as glassy carbon, pyrolytic graphite and graphite [10, 12] exhibit a large background current as a result of reduction of sodium ions to form intercalation compounds before aluminium deposition begins.

2. Experimental details

The required quantities of synthetic cryolite, 4 wt % alumina and aluminium fluoride (all supplied by Comalco Ltd, Bell Bay, Tasmania, Australia) or sodium fluoride (Laboratory grade, Ajax Chemicals, Sydney, Australia) were pre-mixed to ensure homogeneity on melting, and introduced into a carbon crucible (AGSX grade, Carbon Brush manufacturing Pty. Ltd, Sydney, Australia) with dimensions 45 mm i.d. × 52 mm o.d. × 140 mm inside × 150 mm outside. The crucible was also fitted with a carbon lid. The chemicals had been vacuum dried for 24 h at 200° C. The crucible and its contents were placed in the isothermal zone of a vertical Kanthal resistance furnace and heated up slowly (150–200° C h^{-1}) under an inert atmosphere of dry argon.

The working electrode was a tungsten wire electrode (Alfa Products, Danvers, MA 01923, USA). The tungsten wire was 1 mm in diameter and it was immersed 15 mm into the electrolyte, giving an electrode area of 0.48 cm^2. The depth of immersion could be accurately controlled because the mass of electrolyte was calculated such that its liquid volume would fill the crucible to a depth of 30 mm. The surface of the electrolyte could also be detected when lowering the tungsten electrode, using a voltmeter.

A similar tungsten wire electrode was used as a quasi-reference electrode. The carbon crucible served as the counter electrode. All the electrodes were placed in position before heating up the furnace.

The melt temperature was measured with a chromel–alumel thermocouple (Pyrosales, Sydney, Australia) and was maintained at 1031 ± 3° C for all the experiments. For each set of experiments (one melt composition), the temperature varied only by ± 1° C.

The melt was studied using cyclic voltammetry (CV) and current reversal chronopotentiometry (CRC) with and without a delay time introduced between the forward and reverse current pulses. The potential or current functions were generated and controlled by an EG&C PARC Model 175 Universal Programmer and PAR Model 173 Potentiostat/Galvanostat. The resulting voltammogram (*I–E* curve) or chronopotentiogram (*E–t* curve) was recorded on a Riken–Denshi Model D-8DG *X–Y* recorder.

3. Results

3.1. *Cyclic voltammetry*

A background scan of NaF and 4 wt % Al_2O_3 is shown in Fig. 1. Since liquid sodium boils at 1156 K [1], sodium gas is evolved at the cathode at 1304 K in our experiments. Thus stripping of Na was not observed, instead a small peak due to reoxidation of dissolved sodium was observed at − 0.5 V.

In the presence of large amounts of AlF_3, aluminium is deposited, as shown by the cathodic current region A–B–C and its subsequent stripping, *viz.* anodic peaks C′, B′ and A′ (Fig. 2). Cathodic peak A is due to the formation of W–Al alloy and stripping of this alloy is shown by a broad anodic peak A′, the result of a number of W–Al alloys. The deposition of pure liquid aluminium on top of the W–Al alloys is indicated by B and C in Fig. 2.

The shapes of the cyclic voltammograms for melts of increasing cryolite ratio are essentially the same (Figs 2–4). However, cathodic peak A becomes less well defined and the cathodic current in the A–B region increases more rapidly showing the effect of sodium co-deposition superimposed on aluminium deposition (compare Figs 1, 2 and 4).

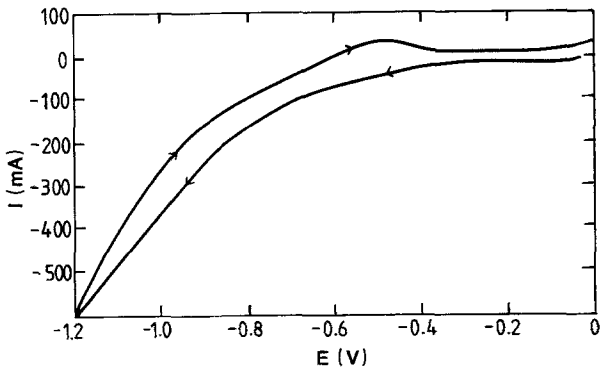

Fig. 1. Cyclic voltammogram of NaF + 4 wt % Al_2O_3 at 1016° C and v = 50 mV s^{-1}.

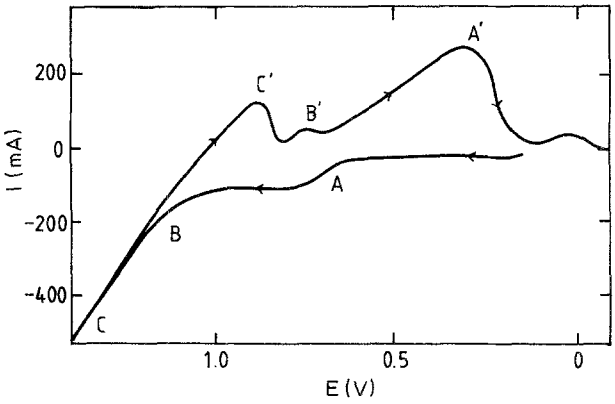

Fig. 2. Cyclic voltammogram of melt with CR = 1.45 and 4 wt % Al_2O_3 at 1026° C and $v = 50\,mV\,s^{-1}$.

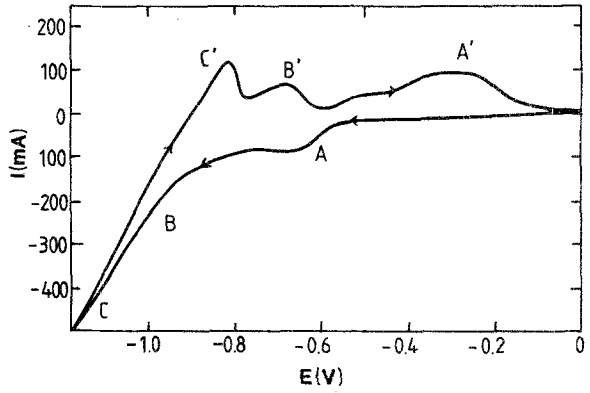

Fig. 4. Cyclic voltammogram of melt with CR = 4.3 and 4 wt % Al_2O_3 at 1029° C and $v = 50\,mV\,s^{-1}$.

The peak potentials observed in cyclic voltammetry correspond to the quarter-wave potentials of identical reactions in chronopotentiometry. Chronopotentiograms for melts of the same compositions as those studied by CV are shown in Fig. 5.

3.2. *Current reversal chronopotentiometry*

Figure 5a shows a current reversal chronopotentiogram (CRC) corresponding to the deposition and reoxidation of aluminium at a tungsten electrode in a cryolite melt (CR = 3) containing 4 wt % Al_2O_3. During the cathodic pulse, the potential is seen to rise fairly sharply to approx. -1.0 V where AlF_6^{3-} ions [1–3] are reduced to Al(l). On reversal of the current, two reverse transitions are observed, the first τ_{r2}, corresponding to the reoxidation of aluminium metal, while the second, τ_{r1}, is ascribed to the reoxidation of the Al–W alloy formed at the interface between the deposited metal and the substrate.

A CRC obtained under similar conditions in a basic melt (CR = 4.3) is shown in Fig. 5b. During the forward cathodic pulse, the potential rises more gradually to approximately -1.0 V, probably due to Na metal co-deposition. On reversal of the current, a third reverse transition, τ'_{r2}, is sometimes observed and is probably associated with the reoxidation of sodium.

A CRC in an acidic melt (CR = 0.8) is shown in Fig. 5c and a cathodic prewave can be observed at approximately -0.95 V. On reversal of the current, two reverse transitions are again observed in Fig. 5c, τ_{r2} corresponding to aluminium metal reoxidation, while τ_{r1} is due to the reoxidation of the Al–W alloy.

This prewave is observed clearly in acidic melts (CR < 3) but not in basic melts (CR > 3), although the corresponding cathodic peak in cyclic voltammetry is observed for all CRs (Figs 2–4). Further evidence that this prewave is an insoluble W–Al alloy is shown in Fig. 6. Reversing the current just after τ_{f1} results in τ_{r1}/t_f being close to 1. if τ_{r1} were due to the oxidation of dissolved metal, τ_{r1}/t_f would be one-third [13].

The total amount of aluminium and alloy (and Na) stripped during the reverse anodic pulse is thus given by the sum of the reverse transitions ($\tau_r = \tau_{r1} + \tau_{r2}\,(+\tau'_{r2})$). If there were no metal loss due to a dissolution reaction, the ratio of τ_r/t_f (where t_f is the forward electrolysis time) should be equal to 1. In each of Figs 5a–c, however, τ_r/t_f is less than one, indicating that a dissolution process is occurring, resulting in metal loss. The rate of metal dissolution can be calculated from the ratio τ_r/τ_f as shown below.

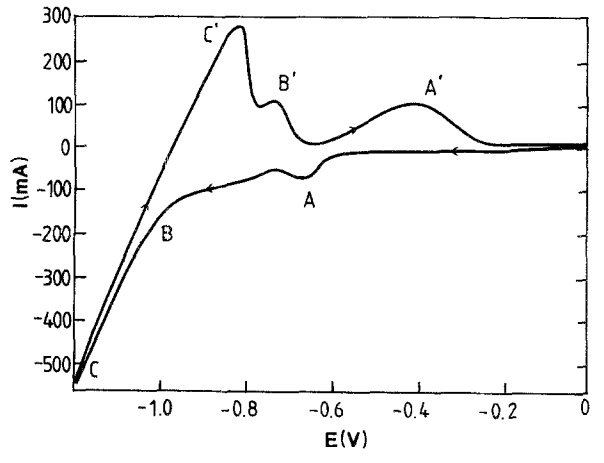

Fig. 3. Cyclic voltammogram of melt with CR = 3 and 4 wt % Al_2O_3 at 1030° C and $v = 50\,mV\,s^{-1}$.

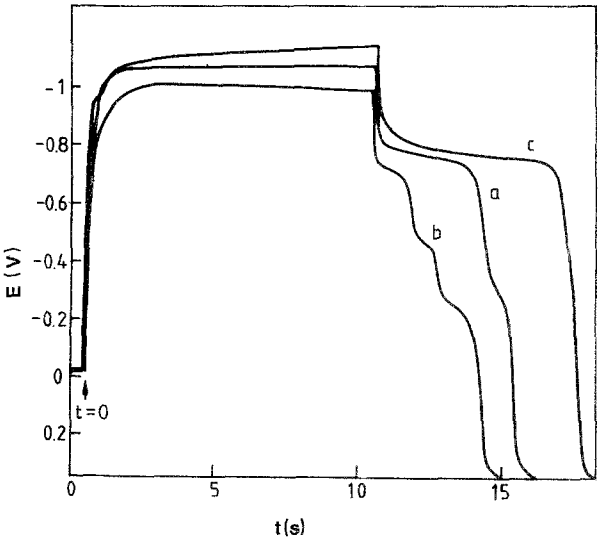

Fig. 5. CRC: $I = 300$ mA, $t_f = 10$ s. (a) CR = 3 (1030° C), (b) CR = 4.3 (1029° C), (c) CR = 0.8 (1034° C).

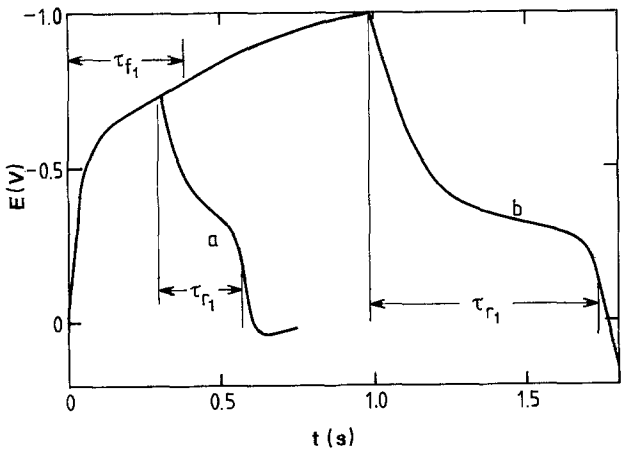

Fig. 6. CRC: I = 300 mA, (a) t_f = 0.3 s and (b) t_f = 1 s. Cryolite melt with CR = 1.45 and 4 wt % Al_2O_3 at 1026° C.

Mass balance on Al gives

$$\text{Al deposited} = \text{Al dissolved} + \text{Al stripped}$$

$$\frac{I_f}{AnF} t_f = r_d[t_f + \tau_r] + \frac{I_r}{AnF} \tag{3}$$

where r_d is the rate of dissolution.

$$r_d = \frac{I_f t_f - I_r \tau_r}{AnF[t_f + \tau_r]}$$

since $I_f = I_r$

$$r_d = \frac{I_f\left[1 - \frac{\tau_r}{t_f}\right]}{AnF\left[1 + \frac{\tau_r}{t_f}\right]} \text{ mol cm}^{-2}\text{s}^{-1} \tag{4}$$

Expressing $r_d = I_d/AnF$, where I_d is the 'dissolution current',

$$I_d = \frac{I_f\left[1 - \frac{\tau_r}{t_f}\right]}{\left[1 + \frac{\tau_r}{t_f}\right]} \tag{5}$$

The metal dissolution rate, r_d, was thus calculated from the limiting value of R_1 which is measured from a plot of $R = (\tau_{r1} + \tau_{r2})/t_f$ against t_f

$$r_d = \frac{I(1 - R_1)}{AnF(1 + R_1)} \text{ mol cm}^{-2}\text{s}^{-1} \tag{6}$$

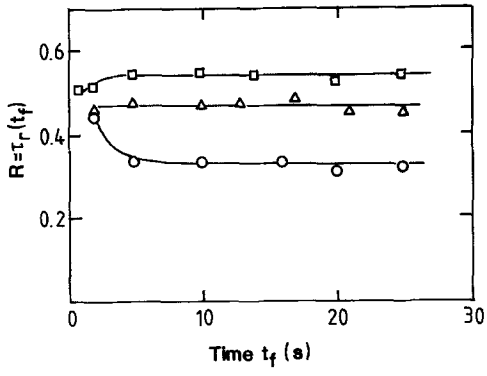

Fig. 7. Cryolite melt with CR = 3 and 4 wt % Al_2O_3 at 1030° C. Plot of $(\tau_{r1} + \tau_{r2})/t_f$ vs t_f for various current densities. (○) 200 mA; (△) 300 mA; (□) 400 mA.

where I = current applied (A)
R_1 = limiting transition time ratio
A = area of electrode (cm^2)
n = number of electrons
F = Faraday's constant ($C\,mol^{-1}$).

A large number of CRCs were obtained for various values of t_f and at different current densities and CRs. Figure 7 shows plots of τ_r/t_f vs t_f at three different current densities for a cryolite melt containing 4 wt % Al_2O_3. The high values of τ_r/t_f at small t_fs and low current densities is probably due to the fact that at short electrolysis times there is mainly alloy formation on the electrode surface which is less soluble in the melt than liquid aluminium. At longer electrolysis times, the surface is covered in liquid aluminium, so that a decreased ratio of τ_r/t_f is expected due to its higher dissolution rate. At higher current densities (e.g. I = 400 mA or i = 0.8 A cm^{-2}) the effect of the alloy is eliminated very quickly because liquid Al is deposited faster. Hence the decreasing trend at short t_fs is not observed.

The metal dissolution rate was calculated from CRCs over a range of current densities and at various CRs and the results are summarized in Table 1.

3.3. *Current reversal chronopotentiometry with delay*

Current reversal chronopotentiometry with delay was also used to calculate the metal dissolution rate. In these experiments, the amount of charge passed during the cathodic pulse was kept constant at Q = 8000 mC for all current densities. The current was then switched to zero for various delay times, t_d, before an anodic pulse was applied to reoxidize the metal on the electrode surface.

A typical CRC with delay is given in Fig. 8. The ratio τ_r/t_f is plotted as a function of t_d and a decreasing trend was observed for all current densities and all compositions. Figure 9 shows the linear plot of τ_r/t_f vs t_d for a cryolite melt with 4 wt % Al_2O_3. The metal dissolution rate can be calculated from the slope of these plots as follows:

The amount of metal deposited during t_f corresponds to the amount of charge Q_f where

$$Q_f = I_f t_f$$

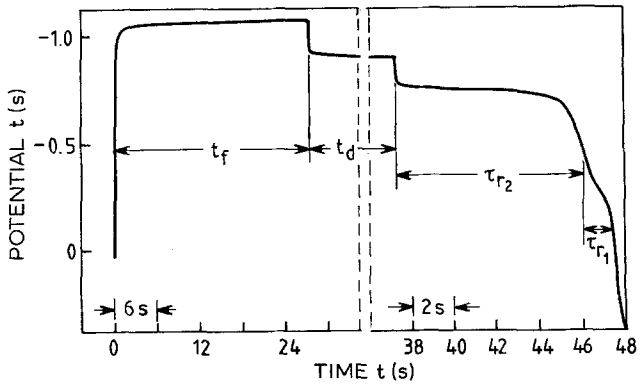

Fig. 8. CRC with delay for cryolite melt with CR = 3 and 4 wt % Al_2O_3 at 1029° C. I = 300 mA, t_f = 26.7 s and t_d = 10 s.

Table 1. NaF–AlF_3–4 wt % Al_2O_3 system

Cryolite ratio CR	*Temperature t (°C) (a) CRC (b) Delay*	*Current density i ($A\,cm^{-2}$)*	*Dissolution rate ($10^{-7}\,mol\,cm^{-2}\,s^{-1}$) r_d*		*Mean r_d*	
			CRC	*Delay*	*CRC*	*Delay*
0.8	(a) 1034 ± 2	0.4	3.332	2.022		
	(b) 1034 ± 2	0.6	–	2.637	3.332	2.609
		0.8	–	3.169		
1.45	(a) 1026 ± 2	0.4	4.421	–		
	(b) 1026 ± 2	0.6	5.230	4.672	5.113	5.142
		0.8	5.688	5.613		
2.0	(a) 1033 ± 1	0.4	6.391	4.328		
	(b) 1033 ± 1	0.6	6.540	5.355	6.747	5.096
		0.8	7.309	5.606		
2.6	(a) 1031 ± 1	0.4	7.631	5.857		
	(b) 1031 ± 1	0.6	8.521	6.515	8.642	6.283
		0.8	9.775	6.476		
3	(a) 1030 ±1	0.4	7.267	4.58		
	(b) 1029 ± 1	0.6	7.784	5.007	7.891	5.065
		0.8	8.622	5.607		
4.3	(a) 1029 ± 1	0.4	9.595	7.716		
	(b) 1029 ± 1	0.6	11.934	7.787	11.558	8.389
		0.8	13.145	9.665		
5.7	(a) 1035 ± 1	0.8	25.37	15.237		
	(b) 1035 ± 1	1	26.69	12.278	26.03	13.572
		1.2		13.2		

After delay time t_d, the amount of Al remaining is represented by

$$\begin{aligned} Q_r &= \tau_r I_r \\ &= \tau_r I_f \quad \text{since} \quad I_f = I_r \\ &= \frac{\tau_r}{t_f} Q_f \end{aligned}$$

For a constant rate of dissolution, r_d, the relationship between τ_r/t_f and t_d is linear. Choose t_{d1} and t_{d2} where $t_{d2} > t_{d1}$. During time interval $(t_{d2} - t_{d1})$, moles Al dissolved is given by

$$m_d = \frac{\tau_{r_{d_2}} - \tau_{r_{d_2}}}{t_f} \times \frac{Q_f}{nF}$$

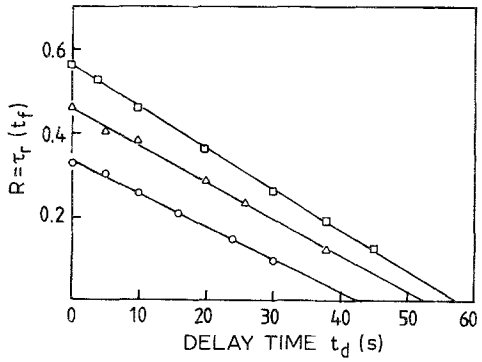

Fig. 9. Cryolite melt with CR = 3 and 4 wt % Al_2O_3 at 1029° C. Plot of $(\tau_{r1} + \tau_{r2})/t_f$ vs t_d for various current densities. (○) 200 mA; (△) 300 mA; (□) 400 mA.

Hence, the rate of dissolution, r_d, is given by

$$r_d = \frac{m_d}{t_{d2} - t_{d1}} = \frac{m_d}{\Delta t_d}$$

$$r_d = \frac{\Delta\left[\frac{\tau_r}{t_f}\right]}{\Delta t_d} \times \frac{Q_f}{AnF} \text{ mol cm}^{-2}\text{s}^{-1} \qquad (7)$$

for an electrode area of $A\,cm^{-2}$.

The dissolution rate r_d is thus obtained from the slope, b, of the τ_r/t_f vs t_d plot

$$r_d = b\,\frac{Q_f}{AnF} \text{ mol cm}^{-2}\text{s}^{-1} \qquad (8)$$

Values of r_d were calculated from delay data obtained at a range of current densities and cryolite ratios and the results are summarized in Table 1. The dissolution rates obtained by both CRC and delay are plotted as a function of CR in Fig. 10 and an inflexion is observed in both plots around CR = 3.

4. Discussion

The inflexion in Fig. 10 indicates a change in the dissolution mechanism when the melt composition changes from being acidic (CR < 3) to basic (CR > 3). Alternatively, it may be more correct to say that there are two dissolution reactions but one predominates depending on the cryolite ratio.

In general, the dissolution rates obtained from CRC experiments were higher than those from CRC with delay experiments, the difference increasing for higher

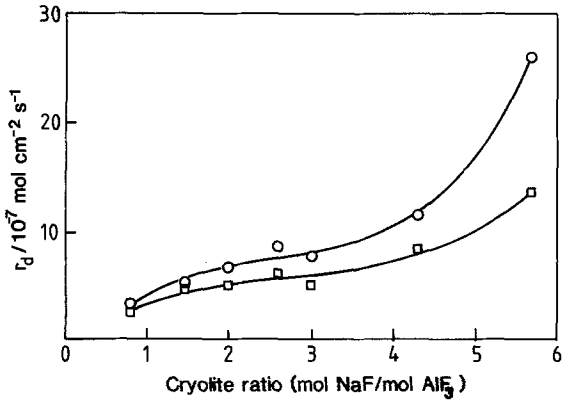

Fig. 10. Dissolution rate of Al as a function of cryolite ratio at 1031 ± 3° C. (○) CRC; (□) Delay.

cryolite ratios. There are two reasons for this observation. The first is that CRC experiments are conducted at short electrolysis times, i.e. less than 25 s. Therefore, the dissolution rate measured is actually the initial dissolution rate under non-steady state conditions.

During aluminium deposition, the cryolite ratio is actually higher at the electrode surface than in the bulk of the electrolyte. The actual cryolite ratio at the cathode depends on the current density and hydrodynamic conditions. For example, if the bulk cryolite ratios were 1, 3 and 4, then the corresponding cryolite ratios at the electrode surface would be 1.25, 6 and 7.3, respectively, for an unstirred melt and a current density of 0.6 A cm^{-2} [14]. The second reason is that current efficiency with respect to aluminium deposition varies with cryolite ratio [1–3]. As the CR increases, the current efficiency decreases. According to Lozhkin and Popov [15], simultaneous discharge of aluminium and sodium cations begins at CR = 2.8 in cryolite–alumina melts. Hence, the apparently greater increase in dissolution rate at high cryolite ratios in CRC experiments is partly attributable to more co-deposition of sodium. Since the fraction of cathodic charge which results in aluminium deposition is smaller, the stripping time, τ_{r2}, consequently also becomes smaller resulting in a lower ratio of $(\tau_{r1} + \tau_{r2})/t_f$, even if the dissolution rate of aluminium were not cryolite-ratio dependent.

The results obtained using the method of CRC with delay were not influenced by the co-deposition of sodium where this may have occurred. The amount of aluminium remaining on the electrode (represented by $\tau_{r1} + \tau_{r2}$) was measured as a function of delay time. Regardless of the current efficiency of the cathodic process, the amount of aluminium deposited was the same within each set of experiments, delay time being the only variable. The CRC with delay results were obtained under steady state conditions since the delay times used exceeded 20 s. Hence, the dissolution rate of aluminium under open circuit conditions was measured more accurately using the CRC with delay method. Dissolution rate would be different under electrolysis conditions because of different local conditions at the cathode.

Bersimenko and Vetyukov showed that the rate of aluminium loss increased with cryolite ratio for the range $1.7 < CR < 3.1$ [6]. The results of Duruz and Landolt [8] in cryolite (CR = 3 without Al_2O_3) gave a corrosion current of 40 mA cm^{-2} which is equivalent to 13.4 mg cm^{-2} h^{-1}. They also reported that the dissolution rate (represented by anodic charge/cathodic charge in galvanostatic pulse reversal experiments) increased with increasing CR for the range $2 < CR < 7$. In comparison with other workers (Table 2), we obtained a dissolution rate of 5.065×10^{-7} mol cm^{-2} s^{-1} or 49.2 mg cm^{-2} h^{-1} in cryolite–4 wt % Al_2O_3 (CR = 3, 1030° C). This value is higher than those reported in the literature but it is of the same order of magnitude. Our melt temperature was 30–50° C higher than those used by other workers. Furthermore, the effect of alumina on the rate of dissolution of aluminium is unclear at this point in time. Alumina may affect the deposition and dissolution reactions indirectly through its interaction with AlF_6^{3-} ions [2], e.g.,

$$4AlF_6^{3-} + Al_2O_3 \longrightarrow 3Al_2OF_8^{4-} \quad (9)$$

or

$$4AlF_6^{3-} + Al_2O_3 \longrightarrow 3Al_2OF_6^{2-} + 6F^- \quad (10)$$

In their studies on aluminium saturation solubility as

Table 2. Rates of dissolution of aluminium

Workers	*Rate of Al dissolution (mg cm^{-2} h^{-1})*	*Temperature (° C)*	*Electrolyte (unstirred) composition*
Bersimenko and Vetyukov (1967)	3.97	985	Cryolite–5 wt % Al_2O_3 CR = 2.8
Bersimenko and Vetyukov (1967)	30	970	Cryolite–5 wt % Al_2O_3 CR = 3
Oblakowski and Orman (1973)	4.6	1000	Cryolite–10 wt % Al_2O_3
Duruz and Landolt (1985)	13.4	1000	Cryolite only CR = 3
This work (1988)	49.2	1030	Cryolite–4 wt % Al_2O_3 CR = 3
	37.3	1030	Cryolite only CR = 3

a function of cryolite ratio, Yoshida *et al.* [16] and Odegard *et al.* [17] observed a similar trend, i.e. for $1 < CR < 4$, the saturation concentration of dissolved aluminium increased monotonically and then levelled off at around $CR = 3$. We observed the same trend for the rate of dissolution vs the cryolite ratio (Fig. 10). Assuming diffusion through the metal/melt boundary layer is rate determining, this similarity would be expected because

$$r_d = \frac{D(C_{x=0} - C_{x\to\infty})}{\delta} \quad (11)$$

where r_d = rate of alumina dissolution (mol cm^{-2} s^{-1})
D = diffusion coefficient of dissolved aluminium (metal) (cm^2 s^{-1})
δ = thickness of diffusion layer at the metal/electrolyte interface (cm)
C_x = concentration of dissolved aluminium (metal) at a distance x from the electrode surface (mol cm^{-3}).

Since $C_{x\to\infty}$ 0, r_d is proportional to $C_{x=0}$. For pure cryolite, we estimated $C_{x=0}$ to be 5.56×10^{-5} mol cm^{-3} (0.07 wt %) based on $r_d = 3.84 \times 10^{-7}$ mol cm^{-2} s^{-1} (experimental value), $D = 6.90 \times 10^{-5}$ cm^{-2} s^{-1} [1] and $\delta = 0.01$ cm [18]. This value of $C_{x=0} = 0.07$ wt % Al agrees very well with the literature data for saturation solubility [1, 17] which fall in the region 0.05–0.1 wt %.

The inflexion in Fig. 10 shows that there are two dissolution mechanisms, one being dominant for $CR < 3$ or $CR > 3$. These reactions are generally presented as [1, 2]:

$$2Al + Al(III) \rightleftharpoons 3Al(I) \quad (12)$$

and

$$Al + 3Na^+ \rightleftharpoons Al(III) + 3Na(0) \quad (13)$$

Qiu *et al.* [19] have also proposed an electrochemical dissolution mechanism of the form

$$Al - e^- \rightleftharpoons Al^+ \quad (14)$$

Their results suggest an anodic dissolution current which ceased when the external cathodic polarization current exceeded 0.28 A cm^{-2}. The dissolution current of 0.28 A cm^{-2} obtained by Qiu *et al.* [19] in a melt with $CR = 2.2$ and 5 wt % Al_2O_3 at 940° C is equivalent to a dissolution rate of 9.67×10^{-6} mol cm^{-2} s^{-1}. This value is higher than our value of 5.096×10^{-7} mol cm^{-2} s^{-1} (Table 1) but it is still within experimental error. Our results can neither support nor dispute this mechanism of electrochemical dissolution.

Molten cryolite is completely dissociated to Na^+ and AlF_6^{3-} ions, and AlF_6^{3-} dissociates further AlF_4^- and F^- (approximately 25% at 1000° C) [2].

$$Na_3AlF_6(s) \xrightarrow{melt} 3Na^+ + AlF_6^{3-} \quad (15)$$

$$AlF_6^{3-} \rightleftharpoons AlF_4^- + 2F^- \quad (16)$$

When AlF_3 is added

$$AlF_3 + F^- \longrightarrow AlF_4^- \quad (17)$$

Hence, adding more AlF_3 (or decreasing CR) lowers $[AlF_6^{3-}]$ and $[F^-]$ and increases $[AlF_4^-]$ [2].

Figure 10 shows that the rate of Al dissolution decreases with decreasing CR. This general observation can be explained in terms of chemical attack of Al by both Al(III) and sodium ions (Equations 12 and 13). However, the inflexion in Fig. 10 leads us to believe that one reaction predominates over the other, depending on the cryolite ratio.

In an acidic melt ($CR < 3$), attack by Al(III) ions is likely. Since the decrease in r_d with decreasing CR in the acidic region corresponds to the lowering of $[AlF_6^{3-}]$, the attacking Al(III) species is AlF_6^{3-} rather than AlF_4^-. Chemical attack by AlF_6^{3-} may be represented by an equation such as:

$$2Al(l) + AlF_6^{3-} \rightleftharpoons 3Al(I)F_x^{(1-x)} + (6 - 3x)F^- \quad (18)$$

where $Al(I)F_x^{(1-x)}$ is a complex, most probably AlF_2^- [1, 2, 16, 17]. The degree of complexing would vary with CR.

Attack by AlF_6^{3-} would account for the inflexion in Fig. 10 at approximately $CR = 3$ because the concentration of AlF_6^{3-} would be at a maximum and change only slightly for $2.5 < CR < 3.5$. If attack by AlF_6^{3-} were the only dissolution reaction, the rate of Al dissolution would decrease for $CR > 3.5$ since $[AlF_6^{3-}]$ would be lowered by the addition of NaF.

For basic melts ($CR > 3$), the dominating dissolution reaction would involve Na^+. One possible reaction is:

$$Al(l) + 3Na^+ + 4F^- \rightleftharpoons 3Na(soln) + AlF_4^- \quad (19)$$

which may be followed by [1, 2]

$$Na(soln) + Na^+ \rightleftharpoons Na_2^+ \quad (20)$$

or

$$Na(soln) \rightleftharpoons Na^+ + e^- \quad (21)$$

Since the concentrations of Na^+ and F^- increase with increasing CR, the rate of dissolution of Al increases accordingly.

5. Conclusion

Current reversal chronopotentiometry with delay is a good technique for measuring the rate of dissolution of electrolytically deposited aluminium. It provides more accurate data than current reversal chronopotentiometry without delay because analysis using CRC with delay does not assume 100% current efficiency for depositing aluminium from $NaF-AlF_3-Al_2O_3$ systems.

In general, the rate of Al dissolution decreased with decreasing cryolite ratios (higher acidity). There are however two mechanisms for Al dissolution which may be represented by equations such as

$$2Al(l) + AlF_6^{3-} \rightleftharpoons 3Al(I)F_x^{(1-x)} + (6 - 3x)F^-$$

and

$$Al(l) + 3Na^+ \rightleftharpoons 3Na(soln) + Al(III)$$

The first mechanism predominates over the second in acidic melts (CR < 3) and vice versa in basic melts (CR > 3). The rate of dissolution of Al at 1031° C is of the order of 10^{-7} mol cm^{-2} s^{-1}.

Acknowledgement

This project was funded by a grant from Comalco Ltd. The authors are grateful to Comalco for providing materials and for permission to publish these results.

References

[1] K. Grjotheim *et al.* 'Aluminium Electrolysis', 2nd edn, Aluminium-Verlag, Dusseldorf (1982).
[2] K. Grjotheim and H. Kvande, 'Understanding the Hall–Heroult Process for Aluminium Production', Aluminium-Verlag, Dusseldorf (1986).
[3] K. Grjotheim and J. J. Welch, 'Aluminium Smelter Technology', Aluminium-Verlag, Dusseldorf (1980).
[4] R. Oblakowski and Z. Orman, *Arch. Hutn.* **18** (1973) 39.
[5] O. P. Bersimenko and M. M. Vetyukov, *Zh. Prikl. Khim.* **40** (1967) 195; *J. Appl. Chem. U.S.S.R. (Eng. Trans.)* **40** (1967) 177.
[6] O. P. Bersimenko and M. M. Vetyukov, *Sov. J. Non-Ferrous Met.* **8** (1967) 71.
[7] O. P. Bersimenko, *Tr. Leningrad Politekh. Inst.* **272** (1967) 73, in *Chem. Abstr.* **70** (1967) 14756h.
[8] J. J. Duruz and D. Landolt, *J. Appl. Electrochem.* **15** (1985) 393.
[9] J. J. Duruz, G. Stehle and D. Landolt, *Electrochim. Acta* **26** (1981) 771.
[10] K. A. Bowman, Doctorate Dissertation, University of Tennessee (1977).
[11] L. F. Mondolfo, 'Aluminium Alloys: Structure and Properties', Butterworths, London (1976) pp. 394–396.
[12] E. Sum and M. Skyllas-Kazacos, unpublished data.
[13] R. K. Jain, H. C. Gaur and B. J. Welch, *J. Electroanal. Chem.* **79** (1977) 211.
[14] J. Thonstad and S. Rolseth, *Electrochim. Acta* **23** (1978) 233.
[15] L. N. Lozhkin and A. P. Popov, *J. Appl. Chem. U.S.S.R. (Engl. Trans.)* **41** (1968) 2277.
[16] K. Yoshida, T. Ishihara and M. Yokoi, *Trans. Met. Soc. AIME* **242** (1968) 231.
[17] R. Odegard, A. Sterten and J. Thonstad, *Light Metals* (1987) 389.
[18] F. Lantelme, D. Damianacos and M. Chemla, *J. Electrochem. Soc.* **127** (1980) 498.
[19] Z. Qiu, N. Fong and K. Grjotheim, *Light Metals* (1983) 357.